DAB2 promotes pulmonary fibrosis and may act as an intermediate between IGF-1R and PI3K/AKT signaling pathways

CHUN-LIAN LIANG, XIU-LI LI, XIAO-JUAN QUAN and LIN ZHANG

Department of Geriatrics, The Second Affiliated Hospital of Xi'an Jiaotong University, Xi'an, Shaanxi 710004, P.R. China

Received September 29, 2022; Accepted February 16, 2023

DOI: 10.3892/etm.2023.11882

Abstract. Idiopathic pulmonary fibrosis (IPF) is a heterogeneous lung disease associated with high mortality. Disabled-2 (DAB2), an adapter protein, regulates cell-fibrinogen adhesion and fibrinogen uptake. DAB2 is differentially expressed in mouse fibrotic lungs induced by bleomycin according to a genome microarray analysis based on Gene Expression Omnibus database. However, the role of DAB2 in IPF has not been revealed. A bleomycin-induced mouse model of pulmonary fibrosis was constructed in the present study. It found that the expression of DAB2 was upregulated in bleomycin-induced fibrotic lung tissue with collagen fiber deposition and pulmonary interstitium thickening. Colocalization of DAB2 with α-smooth muscle actin (SMA) was observed in lung tissue sections. *In vitro,* human lung fibroblast MRC-5 cells were treated with TGF-β1 and the expression of DAB2 was increased. Knockdown of DAB2 suppressed cell proliferation and the expression of α-SMA, collagen I, collagen IV and fibronectin in TGF-β1-treated MRC-5 cells. The phosphorylation levels of PI3K and AKT were suppressed in DAB2-knockdown cells. IGF-1/IGF-1R has been reported to promote pulmonary fibrosis and activate the PI3K/Akt signaling. In the present study, the activation of IGF-1/IGF-1R signaling pathways in bleomycin-induced fibrotic lung tissues were positively associated with DAB2 expression. The phosphorylation level of IGF-1R was increased in MRC-5 cells with TGF-β1 treatment, and DAB2 expression was decreased by silencing of IGF-1R. This suggested that DAB2 might be a downstream target of the IGF-1R pathway and thus induced PI3K/AKT signaling activation and fibrogenesis. The current study demonstrated the importance of DAB2 in pulmonary fibrosis and suggested the potential of IGF-1R/DAB2/PI3K in the pathogenesis of IPF.

Correspondence to: Dr Chun-Lian Liang, Department of Geriatrics, The Second Affiliated Hospital of Xi'an Jiaotong University, 157 Xiwu Road, Xi'an, Shaanxi 710004, P.R. China
E-mail: qlcl751124@126.com

Key words: idiopathic pulmonary fibrosis, disabled-2, fibrogenesis, insulin-like growth factor receptor, PI3K/Akt signaling

Introduction

Idiopathic pulmonary fibrosis (IPF) is a chronic interstitial lung disease characterized by dense collagen accumulation from alveolar epithelial cell damage and high fibroblast proliferation. It can lead to chronic respiratory failure, physical disability, and severe hypoxemia (1,2). The age of onset of IPF was mainly over 50 years old, and male patients were more than female patients in US (3). Unspecific early symptoms lead to delayed diagnosis of IPF for years (4). Current treatments for IPF include supplemental oxygen and anti-fibrotic drugs, such as nintedanib and pirfenidone (5,6). However, the two drugs only modestly reduce the rate of lung function deterioration (7). Despite these treatments, the median 2-3 survival of patients with IPF remains poor (8). Lung transplantation is the only cure for IPF (9), but the shortage of donor organs has resulted in only a minority of patients being able to undergo lung transplants (10). Therefore, the development of new mitigation strategies, treatment methods and therapeutic targets is urgently needed for patients with IPF.

Although the pathological mechanism of IPF has not been elucidated, it is thought to be mediated by various chemokines, growth factors and cytokines (11). It is important to understand the mechanism of these factors in IPF to accelerate the progress of IPF treatment. Insulin-like growth factor (IGF-1) signaling has been found to be involved in the progression of pulmonary fibrosis in human IPF tissues and mouse models in previous studies (12,13). Meanwhile, IGF-1 requires insulin-like growth factor receptor (IGF-1R) to exert its function. The PI3K/Akt/mTOR signaling pathway also plays an important role in pulmonary fibrosis. Growth factors/ligands-mediated stimulation of receptor tyrosine kinases (RTKs) activate phosphatidylinositol-3 kinase (PI3K), which in turn activates protein kinase B (Akt) and mammalian target of rapamycin (mTOR). The mTOR promote collagen synthesis and proliferation in fibroblasts, leading to pulmonary fibrosis (14,15). Therefore, PI3K/Akt/mTOR signaling pathway act as a downstream target of IGF-1/IGF-1R to play a role in promoting pulmonary fibrosis.

Disabled-2 (*DAB2*), a member of the Disabled gene family, encodes a mitogen-reactive phosphoprotein and is widely expressed in human tissues, including kidney, heart, lung, and skin. DAB2 has been reported to regulate cell-cell and cell-fibrinogen adhesion, integrin αIIbβ3 activation, fibrinogen uptake, and be involved in the regulation of

TGF-β and Ras/MAPK/ERK signaling pathways (16-18). Down-regulation of DAB2 inhibits bleomycin-induced skin fibrosis and activation of systemic sclerotic skin fibroblasts in mice (19). Reduced expression of DAB2 protects myocardial cells from apoptosis under myocardial injury (20,21). Differential gene expression analysis of Gene Expression Omnibus (GEO) dataset showed that DAB2 was differentially expressed in fibrotic lung tissues of C57BL/6 mice induced by bleomycin (BLM). In the present study, we established a mouse model of BLM-induced pulmonary fibrosis and showed a significant up-regulation of pulmonary DAB2 *in vivo*. Here, we hypothesized that DAB2 might play an important role in IPF development. This study aims to investigate the specific role and mechanism of DAB2 in pulmonary fibrosis and the involvement of IGF-1R-related signaling pathways.

Materials and methods

Cell culture and transfection. MRC-5 cell line was purchased from Zhong Qiao Xin Zhou biotechnology (Shanghai, China), and cultured in minimum essential medium (MEM) (Solarbio, Beijing, China) containing 10% fetal bovine serum (Tianhang Biotechnology, Zhejiang, China) at 37˚C with 5% CO_2. Specific *DAB2* siRNA and *IGF-1R* siRNA (22) were transfected into MRC-5 cell respectively when the cell density reached 70%. After 24 h for transfection, cells were treated with 10 ng/ml transforming growth factor-β1 (TGF-β1) (Sino Biological, Beijing, China) for 24 h.

Ethical approval and Animal model. Animal procedures were approved by the Ethics Committee of the Second Affiliated Hospital of Xi'an Jiaotong University (Approval No. 2022-781) and complied with the National Research Council's Guide for the Care and Use of Laboratory Animals. Healthy male C57BL/6 mice (6-8 weeks old, 19-21 g) which were purchased from Liaoning changsheng biotechnology (China) with consistent growth status were selected and randomly divided into two groups (6 mice per group). Mice in each group were fed freely at 12 h light/12 h dark, 22±1˚C, and 45-55% humidity. Anesthesia was induced with 2-3% isoflurane and maintained with 1.5-2% isoflurane. BLM (Yuanye Bio-Technology, Shanghai, China) was given intratracheally into mice (2 U/kg), and the control group was given the same amount of saline. After 21 days, the weight of the mice was measured. A human endpoint was defined as a threshold of 20% weight loss. Mice were sacrificed by CO_2 euthanasia in a chamber with a fill rate of 30% of the chamber volume of CO_2 per min.

Immunofluorescence (IF). The cells were fixed in 4% paraformaldehyde (Sinopharm Chemical Reagent, Shanghai, China) for 15 min, then immersed in PBS for 5 min and repeated three times. The cell sections were incubated with 0.1% tritonx-100 at room temperature for 30 min and immersed in PBS to remove 0.1% tritonx-100 (Beyotime Biotechnology, Shanghai, China). Before hatching the primary antibody, the cell sections were immersed in 1% BSA (bovine serum albumin) (Sangon Biotech, Shanghai, China) for 15 min. The dilution ratio of the primary antibody was 1:100, and the condition was 4˚C overnight. After the primary antibody was washed off, the secondary antibody diluted 1:200 was added, and the cells were incubated at room temperature in the dark for 1 h. The nuclei were stained with DAPI (Aladdin Biochemical Technology, Shanghai, China). Finally, half drops of anti-fluorescence quencher were added to the cell sections. After sealing the slices, the staining was observed under a fluorescence microscope (BX53, Olympus, Tokyo, Japan). Primary antibodies of DAB2 (DF7792#) and α-SMA (BF9212#) were purchased from Affinity Biosciences (China), and Cy3-labeled goat anti-rabbit IgG (A27039#, Invitrogen, Carlsbad, CA, USA) was used as the secondary antibodies of DAB2 and α-SMA. The experiment was independently repeated six times, and representative pictures were selected.

The lung tissues were dehydrated with different concentrations of alcohol for corresponding time, and the alcohol concentration were 70% (2 h), 80% (overnight), 90% (2 h), 100% (1 h), and 100% (1 h), respectively. After dehydration, the lung tissues were waxed through, embedded, and sliced. After deparaffinization, the sections were immersed in 95, 85, and 75% ethanol for 1 min each. After removing the alcohol, the sections were subjected to antigen repair at low heat for 10 min, followed by immersion in 1% BSA for 15 min. The antibody was incubated at 4˚C overnight at a dilution ratio of 1:100 for the antibody used and 1:200 for the secondary antibody. At last, the sections were counterstained with DAPI and observed under a fluorescence microscope (BX53). Cy3-labeled goat anti-rabbit IgG was used to detect DAB2, and FITC-labeled goat anti-mouse IgG (ab6785#, Abcam, Cambridge, UK) was used to detect α-SMA. The experiment was independently repeated six times, and representative pictures were selected.

Hematoxylin-eosin staining. After dewaxed to water, the lung tissue sections were put in hematoxylin (Solarbio, Beijing, China) solution for 5 min and soaked in distilled water for 5 min. The sections were put in 1% acid ethanol (99 ml 70% ethanol and 1ml concentrated hydrochloric acid) and stay for 3 sec, then rinsed with tap water for 20 min, and soaked in distilled water for 2 min. The sections were stained with eosin (Sangon Biotech, Shanghai, China) solution for 3 min. Then the stained slides were successively immersed in 75% (2 min), 85% (2 min) and 95% (2 min) ethanol and followed by dehydration, transparent and seal. The staining was observed under a light microscope (BX53).

Masson staining. After dewaxed to water, slices were stained with hematoxylin solution for 6 min and followed by differentiation with 1% acid ethanol for 3 sec. Then the slices were rinsed with running water for 20 min and soaked in distilled water for 2 min. The moisture on the sections was blotted with absorbent paper, and the sections were stained with ponceau red liquid dye acid complex for 1 min, which was prepared as follows: 0.7 g ponceau (Sinopharm Chemical Reagent, Shanghai, China) and 0.3 g acid fuchsin (Sinopharm Chemical Reagent, Shanghai, China) were dissolved in 99 ml distilled water, and 1ml glacial acetic acid was finally added. After staining, the sections were washed with 0.2% glacial acetic acid aqueous solution (0.2 ml glacial acetic acid and 100 ml distilled water). Subsequently, 1% phosphomolybdic acid solution was dropped for differentiation for 5 min, and the sections

were stained directly with aniline blue solution for 5 min. The aniline blue solution was prepared as follows: 2 g aniline blue was dissolved in 98 ml distilled water, and 2 ml glacial acetic acid was finally added. After staining, the sections were dehydrated, transparent and sealed. The staining was observed under a light microscope (BX53).

Real-time PCR (qPCR). The samples were lysed with 1 ml TRIpure (BioTeke Corporation, Beijing, China) for 5 min. 200 μl chloroform was added to the lysed samples for 3 min at room temperature. After centrifugation, the upper liquid was collected and mixed with the equal volume of isopropanol. Then the mixture was placed at -20˚C overnight. The frozen sample was removed and centrifuged at 4˚C for 10 min. the supernatant was discarded, and the precipitate was allowed to stand for 5 min. Total RNA was obtained by adding 30 μl Rnase-free ddH_2O. Reverse transcription of RNA was performed by BeyoRT II M-MLV reverse transcriptase (Beyotime Biotechnology, Shanghai, China) to obtain cDNA. Real-time PCR reaction system was configured according to 2xTaq PCR MasterMix (Solarbio, Beijing, China) and SYBR Green (Solarbio, Beijing, China) instructions. GAPDH was used as an internal control for normalization. The operating instrument is Exicycler™ 96 (Bioneer Corporation, Daejeon, Korea). The instrument program was as follows: 1) Incubation at 95˚C for 5 min, 2) Incubation at 95˚C for 10 sec, 3) Incubation at 60˚C for 20 sec, 4) Go to line 2, Cycle 40, 5) Incubation at 72˚C, for 2 min 30 sec, 6) Incubation at 40˚C for 1 min, 7) Melting 60˚C to 94˚C, Every 1˚C for 1 sec, 8) Incubation at 25˚C for 1-2 min, 9) Incubation at 72˚C for 30 sec. The primer sequences were as follows: mus-Dab2 F: 5'-CCCTAATGACCCTTGATG-3'; mus-Dab2 R: 5'-GGTGGGAAAGAAGTTGAGA-3'; homo-DAB2 F: 5'-CCCTGAATGGTGATGTTG-3'; homo-DAB2 R: 5'-GGGATAATGGCTATGGAGT-3'; mus GAPDH F: 5'-TGTTCCTACCCCCAATGTGTCCGTC-3'; mus GAPDH R: 5'-CTGGTCCTCAGTGTAGCCCAAGATG-3'; homo GAPDH F: 5'-GACCTGACCTGCCGTCTAG-3'; homo GAPDH R: 5'-AGGAGTGGGTGTCGCTGT-3'.

Western blot (WB). RIPA (Radio Immunoprecipitation Assay Lysis buffer) and PMSF (phenylmethanesulfonylfluoride) (Solarbio, Beijing, China) were used to extract the protein of the samples. The protein concentration was detected by BCA protein concentration determination kit (Solarbio, Beijing, China), and SDS-PAGE was performed by loading 20 μl (10-20 μg) protein onto the gels, which were composed of 5% stacking gel and four different concentrations of separating gels (8, 10, 12, 15%). GAPDH was used as a loading control for normalization. After electrophoresis separation, the protein was transferred to PVDF membrane (Millipore, Billerica, MA, US), and the transferred protein was blocked with 5% skim milk (Sangon Biotech, Shanghai, China). Then the PVDF membrane was incubated with diluted antibody and washed six times with TBST for 5 min each time. ECL chemiluminescence reagent (Solarbio, Beijing, China) was added to the membrane, and the density values of the protein bands were analyzed by Gel-Pro Analyzer 4.0 (Media Cybernetics, Rockville, MD, US). The antibody incubation conditions are shown in Table I.

CCK-8. MRC-5 Cells with and without transfection were seeded in 96-well culture plates with $6x10^3$ cells per well and treated with 10 ng/ml TGF-β1. After 24 h, CCK-8 (Beyotime Biotechnology, Shanghai, China) was added to the cells for 2 h culture, and the OD value of the cells at 450 nm was determined by 800TS enzyme standard instrument (BioTek Instruments, Winooski, VT, US).

Statistical analysis. All data analysis was completed on Graphpad 8.0. Unpaired t-test was used to test the differences between the two groups, and Ordinary One Way ANOVA was used to analyze the gray values of protein bands. Significant post hoc effects were revealed by the Tukey's post hoc test. qPCR results were analyzed by $2^{-\Delta\Delta CT}$ method. All data were presented as mean ± standard deviation (SD) with at least three biological repetitions in each group. P-value less than 0.05 was considered statistically significant.

Results

The expression of DAB2 was significantly up-regulated in the BLM-induced fibrotic lung tissue. Screening of the candidate gene DAB2 was briefly described as following: two datasets from GEO database including GSE42301 and GSE8553 were used for analyzing the differentially up-regulated genes (|Log2 fold change (FC)|>1, P<0.05) in bleomycin-induced fibrotic lungs of C57BL/6 mice. Genes with incomplete annotation information and duplicated genes were removed from this project. There are 30 overlapping genes between GSE8553 and GSE42301. IGF activity is known to maintain human lung homeostasis and involve in relevant pulmonary diseases with an inflammatory component, including pulmonary fibrosis. Previous studies have demonstrated the potential of treating pulmonary fibrosis by targeting IGF-1R. Here, we aim to further investigate the molecular mechanisms involved in IGF-1R signaling in idiopathic pulmonary fibrosis. The differentially down-regulated genes (|Log2 FC|>1, P<0.05) in IGF-1R knockout mice were analyzed based on GEO dataset GSE47065. Only 4 genes (DAB2, TYROBP, FCER1G, and SFRP1) were overlapped among GSE8553, GSE42301 and GSE47065 as shown in the Fig. S1. Genes with known function in lung fibrosis or without any references in regulating fibrosis were not further considered, and thus DAB2 was screen out in this project. Here, in the Fig. 1, we included some data of bioinformatics analysis based on GEO database to support our findings of the differentially expressed DAB2 in pulmonary fibrosis.

The differentially expressed genes in a mouse model of BLM-induced pulmonary fibrosis were identified based on GEO dataset (GSE8553), which contained 4 cases of BLM-induced lung samples (GSM212539, GSM212540, GSM212548, GSM212549) and 2 cases of Saline-treated control samples (GSM212543, GSM212552). After bioinformatics analysis, 244 differentially expressed genes including 74 down-regulated genes and 170 up-regulated genes that met criteria ($|Log_2 FC|>1$, P<0.005) were obtained and showed in a volcano map (Fig. 1A). The chromosomal distribution of these genes was displayed in Fig. 1B. The differentially up-regulated genes were showed by a hierarchical clustering heatmap (Fig. 1C). The pulmonary expression of DAB2 was significantly up-regulated in the BLM group (Fig. 1A-C).

Table I. Conditions of the antibody incubation.

A, Primary antibodies

Name	Cat. no.	Company	Dilution ratio	Conditions
IGF-1 antibody	DF6096	Affinity Biosciences, Ltd.	1:1,000	4˚C overnight
IGF-1R antibody	AF7709	Affinity Biosciences, Ltd.	1:1,000	4˚C overnight
p-IGF-1R antibody	AF4397	Affinity Biosciences, Ltd.	1:1,000	4˚C overnight
DAB2 antibody	bs-5999R	BIOSS	1:1,000	4˚C overnight
Collagen I antibody	A16891	ABclonal Biotech Co., Ltd.	1:1,000	4˚C overnight
Collagen IV antibody	AF0510	Affinity Biosciences, Ltd.	1:1,000	4˚C overnight
Fibronectin antibody	A12932	Affinity Biosciences, Ltd.	1:1,000	4˚C overnight
α-SMA antibody	BF9212	Affinity Biosciences, Ltd.	1:3,000	4˚C overnight
PI3K antibody	AF6241	Affinity Biosciences, Ltd.	1:1,000	4˚C overnight
p-PI3K antibody	AF3242	Affinity Biosciences, Ltd.	1:1,000	4˚C overnight
AKT antibody	AF6261	Affinity Biosciences, Ltd.	1:1,000	4˚C overnight
p-AKT antibody	AF0016	Affinity Biosciences, Ltd.	1:1,000	4˚C overnight
GAPDH	60004-1-Ig	Proteintech Group, Inc.	1:10,000	4˚C overnight

B, Secondary antibodies

Name	Cat. no.	Company	Dilution ratio	Conditions
Goat anti rabbit IgG-HRP	SE134	Beijing Solarbio Science & Technology Co., Ltd.	1:3,000	37˚C 1 h
Goat anti rabbit IgG-HRP	SE134	Beijing Solarbio Science & Technology Co., Ltd.	1:3,000	37˚C 1 h
Goat anti rabbit IgG-HRP	SE134	Beijing Solarbio Science & Technology Co., Ltd.	1:3,000	37˚C 1 h
Goat anti rabbit IgG-HRP	SE134	Beijing Solarbio Science & Technology Co., Ltd.	1:3,000	37˚C 1 h
Goat anti rabbit IgG-HRP	SE134	Beijing Solarbio Science & Technology Co., Ltd.	1:3,000	37˚C 1 h
Goat anti rabbit IgG-HRP	SE134	Beijing Solarbio Science & Technology Co., Ltd.	1:3,000	37˚C 1 h
Goat anti rabbit IgG-HRP	SE134	Beijing Solarbio Science & Technology Co., Ltd.	1:3,000	37˚C 1 h
Goat anti mouse IgG-HRP	SE131	Solarbio (Beijing, China)	1:3,000	37˚C 1 h
Goat anti rabbit IgG-HRP	SE131	Beijing Solarbio Science & Technology Co., Ltd.	1:3,000	37˚C 1 h
Goat anti rabbit IgG-HRP	SE131	Beijing Solarbio Science & Technology Co., Ltd.	1:3,000	37˚C 1 h
Goat anti rabbit IgG-HRP	SE131	Beijing Solarbio Science & Technology Co., Ltd.	1:3,000	37˚C 1 h
Goat anti rabbit IgG-HRP	SE131	Beijing Solarbio Science & Technology Co., Ltd.	1:3,000	37˚C 1 h
Goat anti mouse IgG-HRP	SE131	Beijing Solarbio Science & Technology Co., Ltd.	1:3,000	37˚C 1 h

Herein, pulmonary fibrosis was induced by direct tracheal injection of BLM into the lungs of mice, and an equal volume of normal saline was administered in the same manner as a control (Fig. 1D). HE (Fig. 1E) and Masson (Fig. 1F) staining showed the histopathological changes of the lung, and there was obvious pulmonary fibrosis in the BLM group. The lung index analysis showed that BLM induced a higher lung index (P=0.0002) (Fig. 1G). All above results proved the successful establishment of the mouse model of IPF. After verification by qPCR, we found that the expression level of DAB2 mRNA was significantly increased in BLM group (P<0.0001) (Fig. 1H). The IF staining was observed extensive expression of DAB2 in the BLM group (Fig. 1I). In conclusion, the expression of DAB2 was up-regulated in the BLM-induced pulmonary fibrosis model of mice.

Knockdown of DAB2 inhibited TGF-β1-induced proliferation of MRC-5 cells. In order to clarify the biological function of DAB2, we explored its expression in MRC-5 cells and its effect on cell proliferation. We revealed that the expression of DAB2 was significantly observed in cells treated with TGF-β1 (Fig. 2A), and the relative level of DAB2 mRNA was increased in TGF-β1 group compared with control (Fig. 2B). WB was used to detect protein level of DAB2 in cells transfected with specific siRNA of DAB2 (Fig. 2C, D). The content of DAB2 was found to be significantly decreased in DAB2-knockdown cells with and without TGF-β1 treatment (P<0.0001). After TGF-β1 treatment, it was found that the cell concentration of DAB2-knockdown cells was significantly decreased compared with that of cells transfected with siNC (Fig. 2E).

DAB2-knockdown inhibited fibrogenesis. The results from IF staining revealed that the expression of α-SMA in cells with DAB2 knockdown was significantly reduced compared with cells with siNC (Fig. 3A). In terms of the effect of DAB2

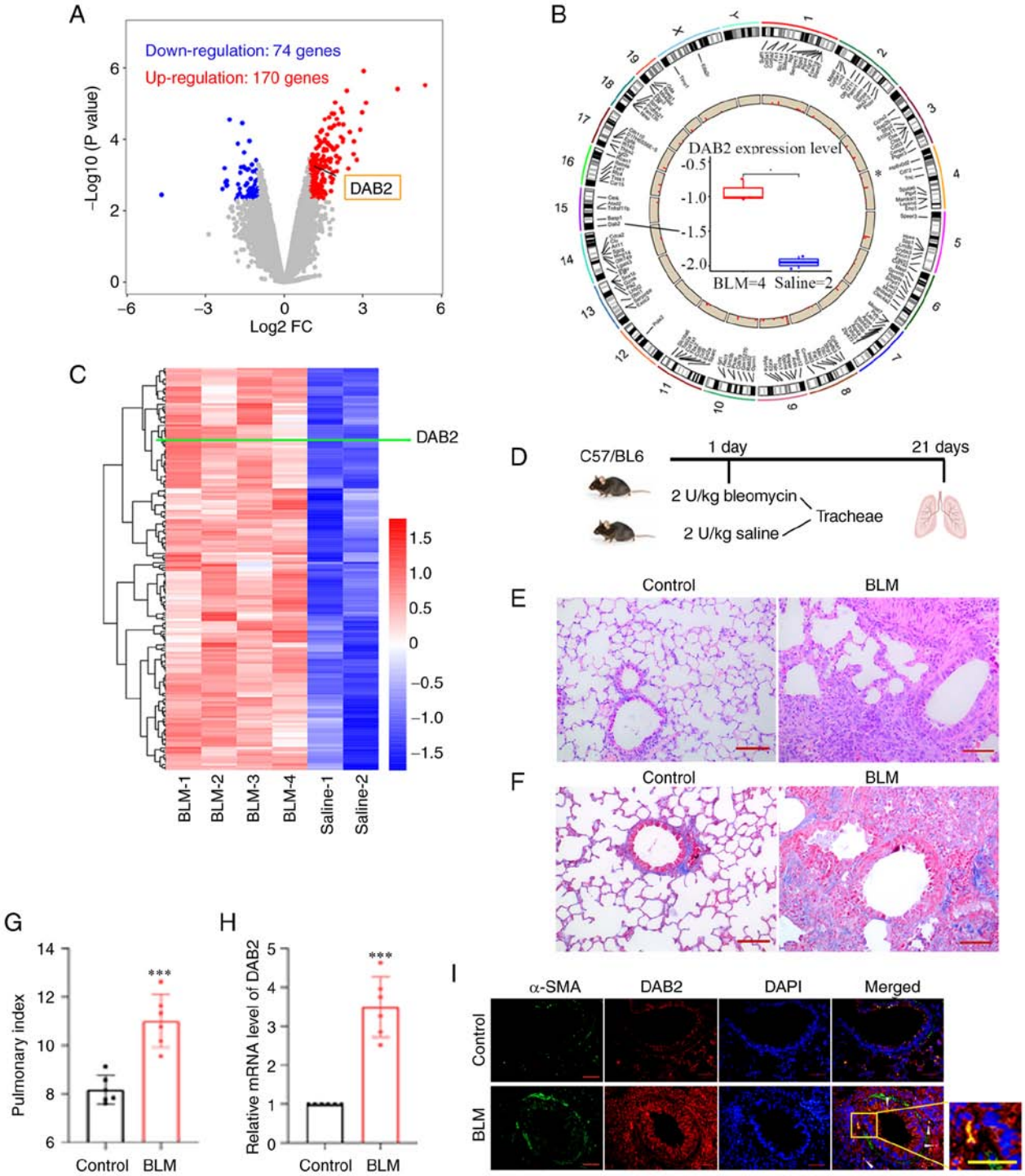

Figure 1. Expression of DAB2 is significantly upregulated in the bleomycin-induced fibrotic lung tissue. (A-C) Results from differential gene expression analysis based on Gene Expression Omnibus database. Lung samples from mice treated with saline (Control group) or bleomycin (BLM group) were set in GSE8553. (A) Volcano plot showing 244 differentially expressed genes with blue dots representing downregulated genes ($Log_2FC<-1$; $P<0.005$) and red dots representing upregulated genes ($Log_2FC>1$; $P<0.005$). (B) Chromosome mapping of these differentially expressed genes including DAB2, which is located on chromosome 15. Boxplot in the center shows the pulmonary expression of DAB2 in Control and BLM mice. $^{*}P<0.05$. (C) Hierarchical clustering heatmap of differentially upregulated genes, in which the row represents genes and the column represents samples. The green line points out the position of DAB2. (D) Schematic diagram of experimental paradigm for bleomycin-induced pulmonary fibrosis model in mice. (E) Hemoxylin and eosin staining of lung tissue sections of mice (scale bar, 100 μm). (F) Masson staining of lung tissue sections of mice (scale bar, 100 μm). (G) Mouse pulmonary index. (H) Relative mRNA level of DAB2 in lung tissues. $^{***}P<0.001$ vs. control. (I) Immunofluorescence staining of lung tissue sections of mice, the white arrow indicates the location where DAB2 is co-expressed with α-SMA (scale bar, 50 μm). Data were presented as mean ± SD with six biological repetitions in each group. DAB2, Disabled-2; FC, fold-change; BLM, bleomycin; SMA, smooth muscle actin.

on fibrogenesis, WB was used to detect the levels of related proteins in the process of fibrosis. We found that the expression of Collagen I, Collagen IV, Fibronectin, and α-SMA in DAB2-knockdown cells was decreased compared with siNC group (Fig. 3B). Therefore, DAB2-knockdown could inhibit fibrogenesis.

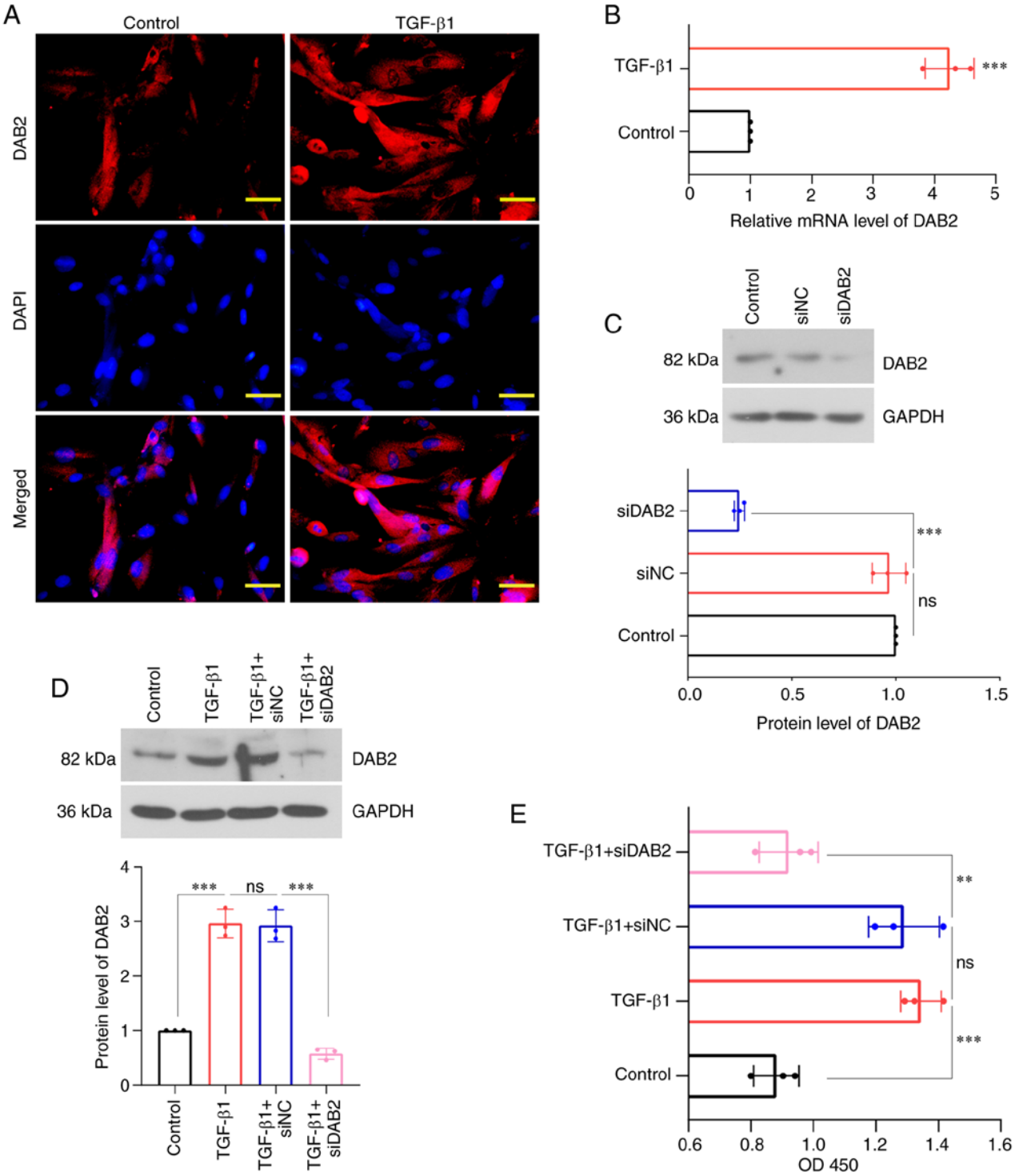

Figure 2. Knockdown of DAB2 inhibits TGF-β1-induced proliferation of MRC-5 cells. Myofibroblast differentiation of MRC-5 cells (human embryonic lung fibroblasts) under TGF-β1 induction for 24 h. (A) Immunofluorescence staining of DAB2 in MRC-5 cells with TGF-β1 treatment (scale bar, 50 μm). (B) Relative mRNA level of DAB2 in TGF-β1-treated MRC-5 cells. ***P<0.001 vs. control (C) Protein level of DAB2 in MRC-5 cells transfected with specific siRNA targeting DAB2. (D) Protein level of DAB2 in MRC-5 cells after transfection of siRNA targeting DAB2 in the presence of TGF-β1. (E) Proliferation of MRC-5 cells was detected by Cell Counting Kit-8. Data were presented as mean ± SD with three biological repetitions in each group. **P<0.01 and ***P<0.00. ns, no significance; DAB2, Disabled-2 actin; si, short interfering; NC, negative control.

Knockdown of DAB2 inhibited PI3K/AKT signaling pathway. A decrease in the phosphorylation levels of PI3K and AKT was found in MRC-5 cells with DAB2 knockdown (Fig. 4). It indicated that knockdown of DAB2 in MRC-5 cells inhibited phosphorylation of PI3K and AKT and thus suppressed PI3K/AKT signaling pathway.

DAB2 might be a downstream target of IGF-1R signaling. In the constructed mouse model, the protein levels of IGF-1, p-IGF-1R and IGF-1R were detected by WB. It revealed that the phosphorylation level of IGF-1R was significantly increased (P<0.001) and protein level of IGF-1 was increased (P<0.001) (Fig. 5A). *In vitro* cell experiments, it was found that the phosphorylation level of

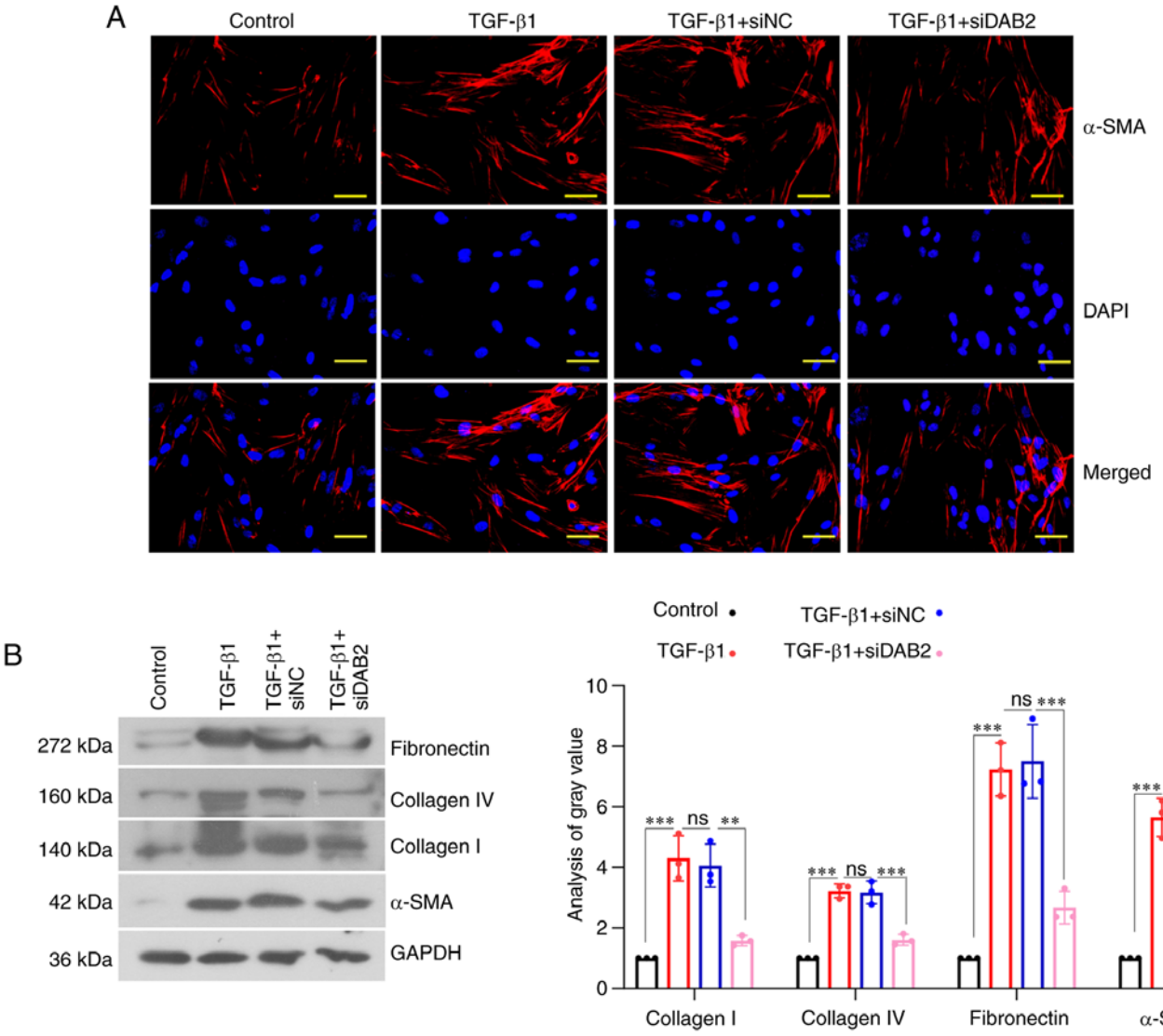

Figure 3. Knockdown of DAB2 inhibited fibrogenesis. (A) Immunofluorescence staining of α-SMA in MRC-5 cells with downregulation of DAB2 following by the treatment of TGF-β1 (scale bar, 50 μm). (B) Protein levels of collagen, collagen IV, fibronectin and α-SMA in the cells. Data were presented as mean ± SD with three biological repetitions in each group. **P<0.01 and ***P<0.001. ns, no significance; DAB2, Disabled-2 actin; SMA, smooth muscle actin; short interfering; NC, negative control.

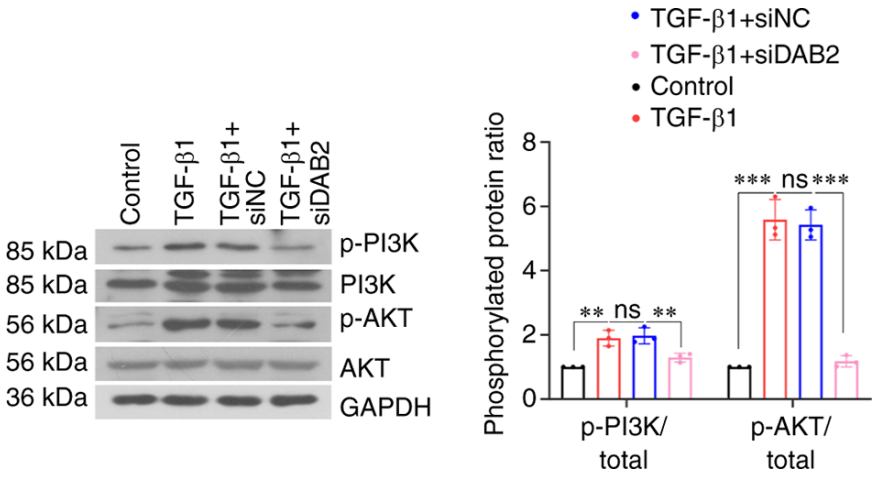

Figure 4. Knockdown of DAB2 inhibits the PI3K/AKT signaling pathway. Western blotting of p-PI3K, PI3K, p-AKT and AKT in DAB2-knockdown MRC-5 cells with the treatment of TGF-β1. The bar plot represents the ratio of phosphorylated versus total protein. Data are presented as mean ± SD with three biological repetitions in each group. **P<0.01 and ***P<0.001. ns, no significance; DAB2, Disabled-2 actin; p-, phosphorylated; si, small interfering; NC, negative control.

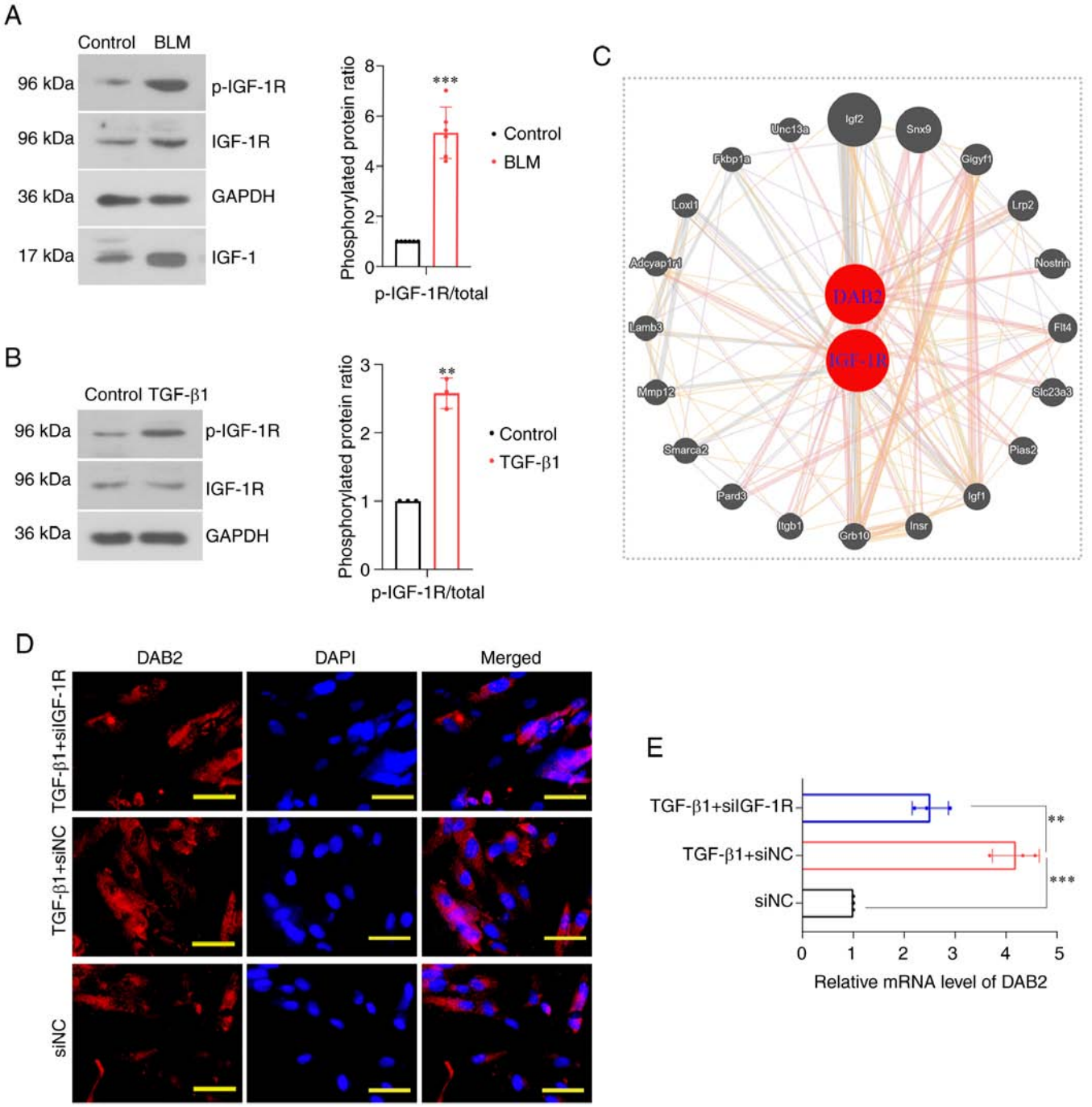

Figure 5. DAB2 may be a downstream target of IGF-1R signaling. (A) Western blotting of IGF-1, p-IGF-1R and IGF-1R, and the ratio of p-IGF-1R vs. total IGF-1R in BLM-induced fibrotic lung tissue (n=6). (B) Western blot analysis of p-IGF-1R and IGF-1R, and the ratio of p-IGF-1R vs. total IGF-1R in MRC-5 cells treated with TGF-β1. **P<0.01 and ***P<0.001 vs. control. (C) Protein-protein interaction network analysis showing the interaction of DAB2 and IGF-1R based on the GeneMANIA database. (D) Immunofluorescence staining of DAB2 in IGF-1R-knockdown MRC-5 cells treated with TGF-β1 (scale bar, 50 μm). (E) Relative mRNA level of DAB2 in IGF-1R-knockdown MRC-5 cells with TGF-β1 treatment. Data are presented as mean ± SD with three biological repetitions in each group. **P<0.01 and ***P<0.001. DAB2, Disabled-2 actin; bleomycin; IGF-1, insulin-like growth factor; IGF-1R, IGF-1 receptor; p-, phosphorylated; si, small interfering.

IGF-1R was increased in cells induced by TGF-β1 (P=0.0012) (Fig. 5B). Protein-protein interaction (PPI) network analysis based on the GeneMANIA database (http://genemania.org/) showed a potential genetic interaction between DAB2 and IGF-1R (Fig. 5C). We further knocked down IGF-1R in MRC-5 cells and examined the expression level of DAB2 in this cell. IF staining showed that the number of positive cells in the IGF-1R-knockdown group was significantly lower than that in the TGF-β1 treatment group without IGF-1R- knockdown (Fig. 5D). QPCR found that the relative mRNA level of DAB2 also decreased (P=0.0021) (Fig. 5E).

Discussion

IPF is one of the most aggressive forms of idiopathic interstitial pneumonia and the most common form of interstitial lung

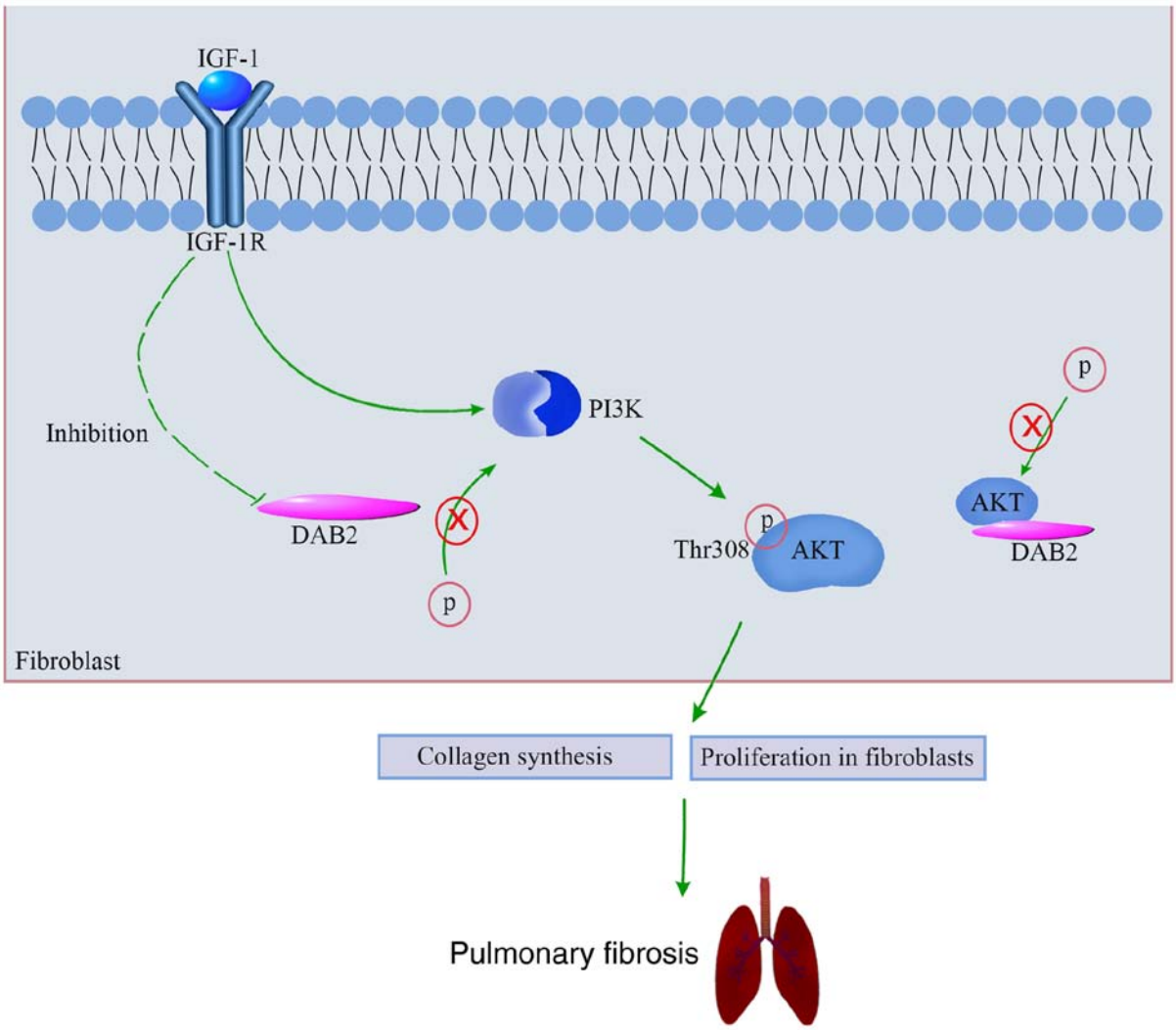

Figure 6. Schematic of the mechanism for DAB2 involvement in PI3K/AKT signaling pathway induced by IGF-1/IGF-1R in fibroblasts. IGF-1/IGF-1R activates the downstream PI3K/AKT signaling pathway, thereby causing collagen production and fibroblast proliferation, which leads to pulmonary fibrosis. The present study found that knockdown of DAB2 inhibited the expression of fibrosis-related genes and proliferation of fibroblasts. In addition, the inhibitory effect of DAB2 on the phosphorylation of PI3K and AKT was also confirmed. Eventually, it was revealed that deletion of IGF-1R suppressed the expression of DAB2. DAB2, Disabled-2 actin; IGF-1, insulin-like growth factor; IGF-1R, IGF-1 receptor; p, phosphate.

diseases, resulting in decline in lung function and progressive respiratory failure (23). Previous studies have found that the pathogenesis of IPF involves numerous growth factors, cytokines and signaling pathways (15), whether these factors can be used as targets for the treatment of IPF and the specific mediator of these signaling pathways in IPF have been the focus of contemporary research.

In studies on fibrotic diseases (19,24), the regulatory effect of DAB2 on fibrogenesis has been revealed. In this study, we will initially reveal the important role of DAB2 in pulmonary fibrotic diseases. DAB2 expression has been shown to be upregulated in skin fibrosis models (19). Herein, we confirmed the up-regulation of DAB2 expression in BLM-induced pulmonary fibrosis in mouse. *In vitro*, we observed that the deletion of DAB2 caused the down-regulation of fibrosis marker genes, indicating that DAB2 may play an important role in pulmonary fibrosis. From the above elaboration, we predict that the expression of DAB2 is up-regulated in fibrotic tissues, and the degree of fibrosis and the expression of related genes were significantly inhibited after knockdown of DAB2. It further presumes that the general inhibitory effect of DAB2 in fibrotic diseases. In addition, most studies have reported the inhibitory effect of DAB2 on cell proliferation (25,26). We found that DAB2-knockdown inhibited the proliferation of MRC-5 cells, which is in agreement with previous research reports.

DAB2, as an adapter molecule, can regulate related signaling pathways to play physiological roles (27). For example, DAB2 can activate TGFβ-R to associate with Smad signaling pathway (18). In the Wnt signaling pathway, DAB2 plays a regulatory role by linking its PTB domain to the domain of Disheveled (28). However, whether DAB2 is involved in IGF-1R-related pathways is still unclear. In addition, numerous studies have reported the pro-fibrotic function of IGF-1/IGF-1R. In a streptozotocin (STZ)-induced mouse diabetes model, activation of IGF-1 induced fibrogenesis in diabetic kidneys, and inhibition of IGF-1R could ameliorate tubelointerstitial fibrosis (29). Deficiency of IGF-1R attenuated the acute inflammatory response in bleomycin-induced lung injury (30). IGF-1R-deficient mice exhibited an improved degree of pulmonary fibrosis (31). In our study, we found

that IGF-1 and IGF-1R were upregulated in BLM-induced pulmonary fibrosis. It had an elevated phosphorylation level of IGF-1R in vitro. Above all suggested that IGF-1/IGF-1R has a crucial role in pulmonary fibrosis. It was worth mentioning that the same promoting effect of DAB2 and IGF-1/IGF-1R in pulmonary fibrosis led us to speculate the possible interaction mechanism between DAB2 and IGF-1/IGF-1R. Therefore, the interactions between DAB2 and its upstream (and downstream) molecules were explored preliminarily in our study.

While studying the function of DAB2, we found that the phosphorylation levels of AKT was decreased in DAB2-knockdown cells. Interestingly, DAB2 has been reported to bind AKT through proline-rich domain (PRD) (32). Another report revealed it played an essential role in AKT recruitment. AKT is a central mediator in the PI3K-AKT-mTOR signaling pathway and indispensable in this signaling pathway (33). It confirmed that DAB2 is able to regulate this signaling pathway through AKT. However, there is another possibility that DAB2 can directly act on PI3K, since the phosphorylation level of PI3K is significantly inhibited in DAB2-knockdown cells. As described in introduction, IGF-1/IGF-1R can activate this pathway to affect pulmonary fibrosis. In the current study, the results from immunofluorescence staining and real-time PCR showed that the expression level of DAB2 was significantly inhibited in IGF-1R-knockdown cells, suggesting that DAB2 might be positively regulated by IGF-1R. The lack of a more effective quantification, such as flow cytometry, for the difference in DAB2 expression levels might be a limitation of the study. Though microscopy analysis may not be the most effective measurement, the present results clearly showed the difference in DAB2 expression in the absence of IGF-1R. As a consequence, IGF-1R has some effect on DAB2 and PI3K/Akt/mTOR signaling pathway. In the regards of exploring the relationship among them, although the interaction between IGF-1R and DAB2 is still unclear, it is possible that IGF-1/IGF-1R may regulate PI3K/Akt/mTOR signaling pathway through DAB2.

The present work is a preliminary study revealing the potential contribution of DAB2 to the development of IPF. Here, we mainly focused on *in vitro* studies and revealed the profibrotic role of DAB2 in TGF-β1-induced MRC-5 cells, which provides a novel direction for better understanding the pathogenesis of pulmonary fibrosis. This study failed to elucidate the role of DAB2 in IPF *in vivo* and more studies need to be carried out in animal models of pulmonary fibrosis. The lack of clinical samples supporting the expression of DAB2 in IPF is also a limitation of the study. Another innovative discovery of this study is that DAB2 might be regulated by the upstream IGF-1R signaling and intervened the downstream PI3K/Akt signaling, which suggests that IGF-1/IGF-1R may affect pulmonary fibrosis via DAB2-mediated PI3K/AKT signaling. Obviously, our study is far from sufficient to unveil the regulatory mechanisms among DAB2, IGF-1/IGF-1R and PI3K/Akt/mTOR signaling pathway. The underlying mechanisms of DAB2 in IPF and the interaction with IGF-1/IGF-1R signaling pathway need further investigation both *in vitro* and *in vivo*. A knockout mouse model for IGF-1R or DAB2 would be helpful to evidence the role of DAB2 and the potential interaction with IGF-1/IGF-1R in IPF development. Although the absence of IGF-1R or DAB2 knockout mice could be a limitation of the present study, the findings of the present study provide novel insights into the pathogenesis of IPF and a potential therapeutic target for pulmonary diseases, which are of significance for basic and clinical research fields of IPF.

Our results revealed an upregulation of DAB2 in lung tissues of mice with bleomycin-induced pulmonary fibrosis and in TGF-β1-induced MRC-5 cells. *In vitro* studies elucidated that DAB2 could promote the expression of fibrosis-related genes and the proliferation of fibroblasts. It suggests that DAB2 might play an important role in promoting pulmonary fibrosis. In addition, our results showed the activation of IGF-1/IGF-1R signaling in *in vivo* and *in vitro* models of pulmonary fibrosis. We further demonstrated that IGF-1R positively regulated the expression of DAB2, and DAB2 positively regulated the phosphorylation of PKT and AKT *in vitro*. It suggests that DAB2 may act as an intermediate between IGF-1/IGF-1R and PKT/AKT signaling pathway and thus inducing fibrogenesis. A schematic summarizing the mechanism of promoting effect of DAB2 in pulmonary fibrosis is shown in Fig. 6. Our study provides more possibilities for the pathogenesis of pulmonary fibrosis and a new therapeutic target for the treatment of pulmonary fibrosis.

Acknowledgements

Not applicable.

Funding

This research was funded by the Natural Science Basic Research Plan of Shaanxi Province (grant no. 2018JM7076).

Availability of data and materials

The datasets used and/or analyzed during the current study are available from the corresponding author on reasonable request.

Authors' contributions

CLL conceptualized, wrote, reviewed and edited the manuscript, acquired funding and supervised the study. XLL carried out the investigation, experiments and data analysis, and wrote the original draft. XJQ performed the investigation, experiments and data analysis. LZ carried out the experiments and data analysis. CLL and XLL confirm the authenticity of all the raw data. All authors have read and approved the final manuscript.

Ethics approval and consent to participate

The study was approved by the Ethics Committee of the Second Affiliated Hospital of Xi'an Jiaotong University (approval no. 2022-781).

Patient consent for publication

Not applicable.

Competing interests

The authors declare that they have no competing interests.

References

1. Richeldi L, Collard HR and Jones MG: Idiopathic pulmonary fibrosis. Lancet 389: 1941-1952, 2017.
2. Kekevian A, Gershwin ME and Chang C: Diagnosis and classification of idiopathic pulmonary fibrosis. Autoimmun Rev 13: 508-512, 2014.
3. Raghu G, Chen SY, Hou Q, Yeh WS and Collard HR: Incidence and prevalence of idiopathic pulmonary fibrosis in US adults 18-64 years old. Eur Respir J 48: 179-186, 2016.
4. Raghu G, Rochwerg B, Zhang Y, Garcia CA, Azuma A, Behr J, Brozek JL, Collard HR, Cunningham W, Homma S, *et al*: An Official ATS/ERS/JRS/ALAT clinical practice guideline: Treatment of idiopathic pulmonary fibrosis. an update of the 2011 clinical practice guideline. Am J Respir Crit Care Med 192: e3-19, 2015.
5. Adamali HI and Maher TM: Current and novel drug therapies for idiopathic pulmonary fibrosis. Drug Des Devel Ther 6: 261-272, 2012.
6. Bonella F, Stowasser S and Wollin L: Idiopathic pulmonary fibrosis: Current treatment options and critical appraisal of nintedanib. Drug Des Devel Ther 9: 6407-6419, 2015.
7. Shenderov K, Collins SL, Powell JD and Horton MR: Immune dysregulation as a driver of idiopathic pulmonary fibrosis. J Clin Invest 131: e143226, 2021.
8. Sgalla G, Iovene B, Calvello M, Ori M, Varone F and Richeldi L: Idiopathic pulmonary fibrosis: Pathogenesis and management. Respir Res 19: 32, 2018.
9. American Thoracic Society. Idiopathic pulmonary fibrosis: Diagnosis and treatment. International consensus statement. American Thoracic Society (ATS), and the European Respiratory Society (ERS). Am J Respir Crit Care Med 161: 646-664, 2000.
10. Spagnolo P, Tzouvelekis A and Bonella F: The management of patients with idiopathic pulmonary fibrosis. Front Med (Lausanne) 5: 148, 2018.
11. Kelly M, Kolb M, Bonniaud P and Gauldie J: Re-evaluation of fibrogenic cytokines in lung fibrosis. Curr Pharm Des 9: 39-49, 2003.
12. Hernandez DM, Kang JH, Choudhury M, Andrianifahanana M, Yin X, Limper AH and Leof EB: IPF pathogenesis is dependent upon TGFβ induction of IGF-1. FASEB J 34: 5363-5388, 2020.
13. Aston C, Jagirdar J, Lee TC, Hur T, Hintz RL and Rom WN: Enhanced insulin-like growth factor molecules in idiopathic pulmonary fibrosis. Am J Respir Crit Care Med 151: 1597-1603, 1995.
14. Alzahrani AS: PI3K/Akt/mTOR inhibitors in cancer: At the bench and bedside. Semin Cancer Biol 59: 125-132, 2019.
15. Ma H, Liu S, Li S and Xia Y: Targeting growth factor and cytokine pathways to treat idiopathic pulmonary fibrosis. Front Pharmacol 13: 918771, 2022.
16. Tsai HJ and Tseng CP: The adaptor protein Disabled-2: New insights into platelet biology and integrin signaling. Thromb J 14 (Suppl 1): S28, 2016.
17. Cheong SM, Choi H, Hong BS, Gho YS and Han JK: Dab2 is pivotal for endothelial cell migration by mediating VEGF expression in cancer cells. Exp Cell Res 318: 550-557, 2012.
18. Hocevar BA, Smine A, Xu XX and Howe PH: The adaptor molecule Disabled-2 links the transforming growth factor beta receptors to the Smad pathway. EMBO J 20: 2789-2801, 2001.
19. Mei X, Zhao H, Huang Y, Tang Y, Shi X, Pu W, Jiang S, Ma Y, Zhang Y, Bai L, *et al*: Involvement of Disabled-2 on skin fibrosis in systemic sclerosis. J Dermatol Sci 99: 44-52, 2020.
20. Wang BW, Fang WJ and Shyu KG: MicroRNA-145 regulates disabled-2 and Wnt3a expression in cardiomyocytes under hyperglycaemia. Eur J Clin Invest: 48, 2018 doi: 10.1111/eci.12867.
21. Lin CM, Fang WJ, Wang BW, Pan CM, Chua SK, Hou SW and Shyu KG: (-)-Epigallocatechin Gallate Promotes MicroRNA 145 Expression against Myocardial Hypoxic Injury through Dab2/Wnt3a/β-catenin. Am J Chin Med 48: 341-356, 2020.
22. Ma W, Kang Y, Ning L, Tan J, Wang H and Ying Y: Identification of microRNAs involved in gefitinib resistance of non-small-cell lung cancer through the insulin-like growth factor receptor 1 signaling pathway. Exp Ther Med 14: 2853-2862, 2017.
23. Barratt SL, Creamer A, Hayton C and Chaudhuri N: Idiopathic Pulmonary Fibrosis (IPF): An Overview. J Clin Med 7: 201, 2018.
24. Fu L, Rab A, Tang LP, Rowe SM, Bebok Z and Collawn JF: Dab2 is a key regulator of endocytosis and post-endocytic trafficking of the cystic fibrosis transmembrane conductance regulator. Biochem J 441: 633-643, 2012.
25. Tseng CP, Ely BD, Li Y, Pong RC and Hsieh JT: Regulation of rat DOC-2 gene during castration-induced rat ventral prostate degeneration and its growth inhibitory function in human prostatic carcinoma cells. Endocrinology 139: 3542-3553, 1998.
26. Sheng Z, Sun W, Smith E, Cohen C, Sheng Z and Xu XX: Restoration of positioning control following Disabled-2 expression in ovarian and breast tumor cells. Oncogene 19: 4847-4854, 2000.
27. Finkielstein CV and Capelluto DG: Disabled-2: A modular scaffold protein with multifaceted functions in signaling. Bioessays 38 (Suppl 1): S45-S55, 2016.
28. Hocevar BA, Mou F, Rennolds JL, Morris SM, Cooper JA and Howe PH: Regulation of the Wnt signaling pathway by disabled-2 (Dab2). EMBO J 22: 3084-3094, 2003.
29. Dong R, Yu J, Yu F, Yang S, Qian Q and Zha Y: IGF-1/IGF-1R blockade ameliorates diabetic kidney disease through normalizing Snail1 expression in a mouse model. Am J Physiol Endocrinol Metab 317: E686-E698, 2019.
30. Pineiro-Hermida S, Lopez IP, Alfaro-Arnedo E, Torrens R, Iñiguez M, Alvarez-Erviti L, Ruíz-Martínez C and Pichel JG: IGF1R deficiency attenuates acute inflammatory response in a bleomycin-induced lung injury mouse model. Sci Rep 7: 4290, 2017.
31. Chung EJ, Kwon S, Reedy JL, White AO, Song JS, Hwang I, Chung JY, Ylaya K, Hewitt SM and Citrin DE: IGF-1 Receptor signaling regulates type II pneumocyte senescence and resulting macrophage polarization in lung fibrosis. Int J Radiat Oncol Biol Phys 110: 526-538, 2021.
32. Koral K and Erkan E: PKB/Akt partners with Dab2 in albumin endocytosis. Am J Physiol Renal Physiol 302: F1013-1024, 2012.
33. Goldbraikh D, Neufeld D, Eid-Mutlak Y, Lasry I, Gilda JE, Parnis A and Cohen S: USP1 deubiquitinates Akt to inhibit PI3K-Akt-FoxO signaling in muscle during prolonged starvation. EMBO Rep 21: e48791, 2020.